ZIKA

A single mutation in the prM protein of Zika virus contributes to fetal microcephaly

Ling Yuan,[1,2]* Xing-Yao Huang,[3]* Zhong-Yu Liu,[3]* Feng Zhang,[1,2]* Xing-Liang Zhu,[1,2]* Jiu-Yang Yu,[3]* Xue Ji,[3] Yan-Peng Xu,[3] Guanghui Li,[1,2] Cui Li,[1,2] Hong-Jiang Wang,[3] Yong-Qiang Deng,[3] Menghua Wu,[4] Meng-Li Cheng,[3,5] Qing Ye,[3] Dong-Yang Xie,[3,5] Xiao-Feng Li,[3] Xiangxi Wang,[6] Weifeng Shi,[7] Baoyang Hu,[4] Pei-Yong Shi,[8] Zhiheng Xu,[1,2,9]† Cheng-Feng Qin[3]†

Zika virus (ZIKV) has evolved into a global health threat because of its unexpected causal link to microcephaly. Phylogenetic analysis reveals that contemporary epidemic strains have accumulated multiple substitutions from their Asian ancestor. Here we show that a single serine-to-asparagine substitution [Ser^{139}→Asn^{139} (S139N)] in the viral polyprotein substantially increased ZIKV infectivity in both human and mouse neural progenitor cells (NPCs) and led to more severe microcephaly in the mouse fetus, as well as higher mortality rates in neonatal mice. Evolutionary analysis indicates that the S139N substitution arose before the 2013 outbreak in French Polynesia and has been stably maintained during subsequent spread to the Americas. This functional adaption makes ZIKV more virulent to human NPCs, thus contributing to the increased incidence of microcephaly in recent ZIKV epidemics.

Zika virus (ZIKV) was first isolated from a sentinel monkey from Uganda's Zika forest in 1947 and, until its recent emergence in the Americas, was known as an obscure mosquito-borne flavivirus (*1*). In the decades following its discovery, sporadic human ZIKV infections with mild signs and symptoms were reported in a few countries in Africa and Southeast Asia. After several explosive outbreaks in Micronesia in 2007 and French Polynesia in 2013–2014, ZIKV rapidly swept through South and Central America in 2015. Early in 2016, the World Health Organization declared the current ZIKV epidemics a public health emergency of international concern, owing to the unexpected causal link to congenital brain abnormalities, especially microcephaly, during pregnancy (*2*, *3*). Investigations with clinical materials and animal models have provided solid evidence that ZIKV directly targets neuronal progenitor cells (NPCs), leading to microcephaly as well as other severe pathological outcomes (*4*–*9*).

ZIKV contains a positive-sense 11-kb genome RNA that encodes three structural proteins (C, prM, and E) and seven nonstructural proteins. ZIKV strains can be divided into the African and Asian lineages (*10*), and the contemporary strains circulating in Pacific islands and the Americas are likely to have evolved from a common ancestral strain in Southeast Asia (*11*). However, there is serological evidence that ZIKV had been circulating in Southeast Asia for many years (*10*, *12*). Why was microcephaly not recognized earlier? Besides the potential impact of herd immunity and the lack of diagnostics and surveillance in epidemic areas, one plausible hypothesis is that ZIKV has acquired some adaptive mutations to become more virulent to the human fetal brain. Some preliminary results from cell lines indicate strain-specific effects in ZIKV-infected cells (*13*, *14*). Whether contemporary ZIKV strains are more likely to cause severe microcephaly in the fetus remains an open question.

We first investigated the in vivo neurovirulence phenotypes of three contemporary ZIKV strains (MTQ/2015, VEN/2016, and SAM/2016) isolated in 2015–2016 (*6*, *15*, *16*) and compared them with the phenotypes of their Asian ancestral strain (CAM/2010) isolated in Cambodia in 2010 (*17*). We used one-day-old neonatal mice, as this stage of development is analogous to the second trimester of pregnancy in humans. Upon intracerebral injection (*18*, *19*), all three contemporary strains led to 100% mortality in neonatal mice, with typical neurological manifestations such as inactivity, motor weakness, and bilateral hind limb paralysis. By contrast, CAM/2010 killed only 16.7% animals (Fig. 1A). Nevertheless, in vitro cell culture–based studies revealed that the contemporary strain VEN/2016 showed similar growth and plaque characteristics to those of CAM/2010 (fig. S1). These results show that the contemporary strains of ZIKV are more neurovirulent in mice than their ancestral strain CAM/2010.

To determine whether the observed neurovirulence phenotype is directly associated with microcephaly, we further compared the contemporary and ancestral strains in an established mouse embryonic microcephaly model (*4*). Littermate brains were infected with the two ZIKV strains at embryonic day 13.5 (E13.5), which corresponds to infection at the first trimester of pregnancy in humans, a time point that is associated with the development of fetal brain abnormalities (*20*). Inspection of the mice at E18.5 revealed that VEN/2016 infection resulted in brains exhibiting a substantial degree of microcephaly (Fig. 1B), including cortical thinning (Fig. 1C and fig. S2A). The microcephaly phenotype caused by VEN/2016 is comparable to our previous findings (*4*) for another contemporary ZIKV strain, SAM/2016. By contrast, CAM/2010 caused less severe symptoms. Although both viruses predominantly targeted the NPCs as described previously (*4*), VEN/2016 showed significantly enhanced replication in the brain compared with CAM/2010 (fig. S2, B and C). This result was further verified in primary cultured mouse NPCs (mNPCs) (fig. S2D). Specifically, in comparison with CAM/2010, VEN/2016 induced more apoptosis (cells positive for the activated form of caspase 3) in different regions of the brain, as well as the loss of more mature and immature neurons (neurons positive for NeuN and Tbr1, respectively) (fig. S3). Furthermore, we found that VEN/2016 disturbed the proliferation and differentiation of NPCs more significantly than did CAM/2010, as indicated by the substantial decrease in phosphorylated histone H3 (P-H3)–positive cells (Fig. 1D and fig. S4A) and the cell cycle exit index (Ki67$^-$ BrdU$^+$/BrdU$^+$ cells) (fig. S4B). Thus, as compared with the ancestral strain, the contemporary ZIKV strain is more virulent to the mouse brain and causes a more severe microcephaly phenotype in the embryonic brain.

We then sought to identify the genetic determinants for the observed virulence phenotype. Genome sequence alignment, with the ancestral strain CAM/2010 as a reference strain, revealed that contemporary ZIKV strains harbor a number of substitutions of amino acids throughout the genome (fig. S5). We mapped these amino acid substitutions on a maximum likelihood tree (fig. S6) and found a positive correlation between the evolution of ZIKV of the Asian lineage and sampling dates (Fig. 2A). Further coalescent analysis indicated that multiple critical residue substitutions have arisen at different time points before the South American outbreak and have been maintained stably in the contemporary epidemic strains (Fig. 2B and fig. S7). To identify potential virulence determinants, seven mutant viruses [Thr^{106}→Ala^{106} (T106A), S109N, N130S,

[1]State Key Laboratory of Molecular Developmental Biology, Chinese Academy of Sciences (CAS) Center for Excellence in Brain Science and Intelligence Technology, Institute of Genetics and Developmental Biology, CAS, Beijing 100101, China. [2]University of CAS, Beijing 100101, China. [3]Department of Virology, State Key Laboratory of Pathogen and Biosecurity, Beijing Institute of Microbiology and Epidemiology, Beijing 100071, China. [4]State Key Laboratory of Stem Cell and Reproductive Biology, Institute of Zoology, CAS, Beijing 100101, China. [5]Graduate School, Anhui Medical University, Hefei 230032, China. [6]National Laboratory of Macromolecules, Institute of Biophysics, CAS, Beijing 100101, China. [7]Shandong Universities Key Laboratory of Etiology and Epidemiology of Emerging Infectious Diseases, Taishan Medical College, Taian 271000, China. [8]Department of Biochemistry and Molecular Biology and Department of Pharmacology and Toxicology, Sealy Center for Structural Biology and Molecular Biophysics, University of Texas Medical Branch, Galveston, TX 77555, USA. [9]Parkinson's Disease Center, Beijing Institute for Brain Disorders, Beijing 100101, China.
*These authors contributed equally to this work.
†Corresponding author. Email: qincf@bmi.ac.cn (C.-F.Q.); zhxu@genetics.ac.cn (Z.X.)

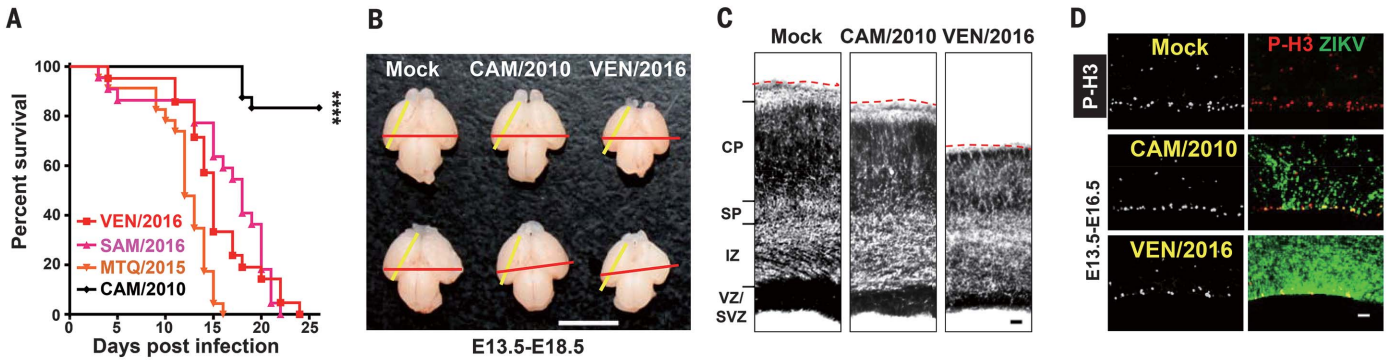

Fig. 1. Neurovirulence phenotypes of the contemporary ZIKV strains and their ancestral Asian strain. (**A**) Neurovirulence tests of different ZIKV strains in neonatal mice. P1 BALB/c mice were intracerebrally injected with 10 plaque-forming units (PFU) of virus, and mortality was observed for 26 days. CAM/2010: n = 24; VEN/2016: n = 21; SAM/2016: n = 22; MTQ/2015: n = 23 (n, number of mice). Log-rank test was performed for statistical analysis. ****P < 0.0001. (**B** to **D**) Littermate embryonic brains were injected with CAM/2010, VEN/2016, or culture media containing 2% fetal bovine serum (mock) at E13.5 and inspected at E16.5 or E18.5. (B) Images of brains (E18.5). Red and yellow bars represent brain width and cerebral cortex length, respectively. (C) Nissl staining of E18.5 brains. CP, cortical plate; SP, subplate; IZ, intermediate zone; VZ, ventricle zone; SVZ, subventricle zone. (D) Images of E16.5 cortices stained with phosphorylated histone H3 (P-H3, red). Scale bars: 5 mm (B), 100 μm (C), 40 μm (D).

S139N, K709R, A982V, and N3144S (S, Ser; N, Asn; K, Lys; R, Arg; V, Val)] were constructed on the basis of the infectious clone of CAM/2010 [wild type (WT)] (fig. S8A), as described previously (*17*). All seven mutant viruses were successfully recovered in BHK-21 cells, and their replication and plaque phenotypes were found to be similar to the WT virus in vitro (fig. S8, B and C). Of all mutants, the S139N mutant virus exhibited the greatest neurovirulence in neonatal mice (Fig. 3A). More importantly, a single reverse substitution, N139S, of the parental virus VEN/2016 significantly decreased mortality caused by the virus in neonatal mice (Fig. 3B and fig. S9). We further characterized the infectivity of the S139N and WT viruses in human NPCs (hNPCs) (fig. S10) derived from human embryonic stem cells (*5*). Our results confirmed that S139N showed enhanced replication in hNPCs (Fig. 3C) and caused more extensive cell death compared with the WT virus (Fig. 3D). Similarly, the S139N mutant showed enhanced viral replication in mNPCs compared with the WT virus (fig. S11A).

Finally, we tested the effect of the S139N substitution in the embryonic microcephaly model. Infection of the S139N mutant virus led to a more severe microcephalic phenotype (Fig. 4A) and thinner cortex (Fig. 4B and fig. S11B) than did infection of the WT virus. Specifically, the S139N mutant virus showed a more robust infection of the NPCs of the embryonic brains (fig. S11, C and D), accompanied by more cell death in the cortical plate (Fig. 4C). Furthermore, the S139N mutant disturbed the NPC proliferation and differentiation more significantly than did the WT virus (Fig. 4D and fig. S12). As expected, the N130S mutant virus caused much less cell death than the S139N mutant in different regions of the brain, similar to the WT virus (fig. S13).

Bioinformatic analysis had identified a panel of substitutions that could have given rise to the different biological phenotypes of ZIKV (*11*, *21*, *22*). However, none of these predications have been validated experimentally. Our results from reverse genetics and mouse neurovirulence studies provide experimental evidence that a single S139N substitution significantly enhances ZIKV infectivity in both human and mouse NPCs and leads to more severe microcephaly in fetal mice. Coalescent analysis indicated that the ZIKV S139N substitution first emerged in May 2013 (95% highest probability density intervals: November 2012 to October 2013), a few months before the 2013 outbreak in French Polynesia (*21*, *23*), and was then stably maintained in the epidemic strain during subsequent spread to the Americas (Fig. 2). The emergence of the S139N substitution correlates with reports of microcephaly and other severe neurological abnormalities, including

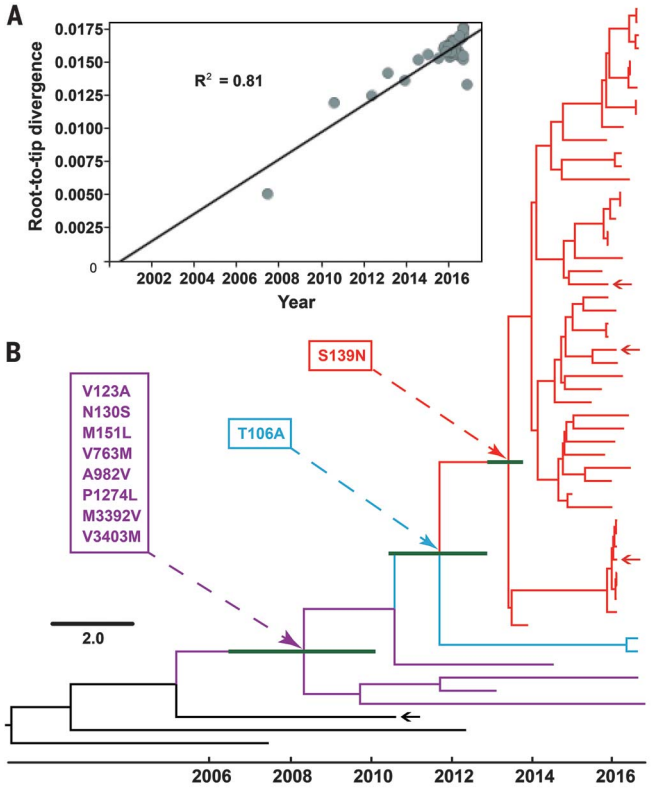

Fig. 2. Phylogenetic and molecular clock analysis of ZIKV strains of the Asian lineage. (**A**) Root-to-tip analysis using TempEst v1.5. The input was a maximum likelihood tree estimated using RAxML (Randomized Axelerated Maximum Likelihood) with 1000 bootstrap replicates (fig. S6). R^2, coefficient of determination. (**B**) Bayesian phylogenetic tree estimated using BEAST v1.8.4. The positions of CAM/2010, VEN/2016, SAM/2016, and MTQ/2015 are indicated with black (CAM/2010) and red (VEN/2016, SAM/2016, and MTQ/2015) arrows. Conserved amino acid changes were inferred using the CAM/2010 strain as the parental strain. The green bars indicate the 95% highest probability density intervals of the age of the lineage. The details of the tree are shown in fig. S7. V, Val; A, Ala; N, Asn; S, Ser; M, Met; L, Leu; P, Pro; T, Thr.

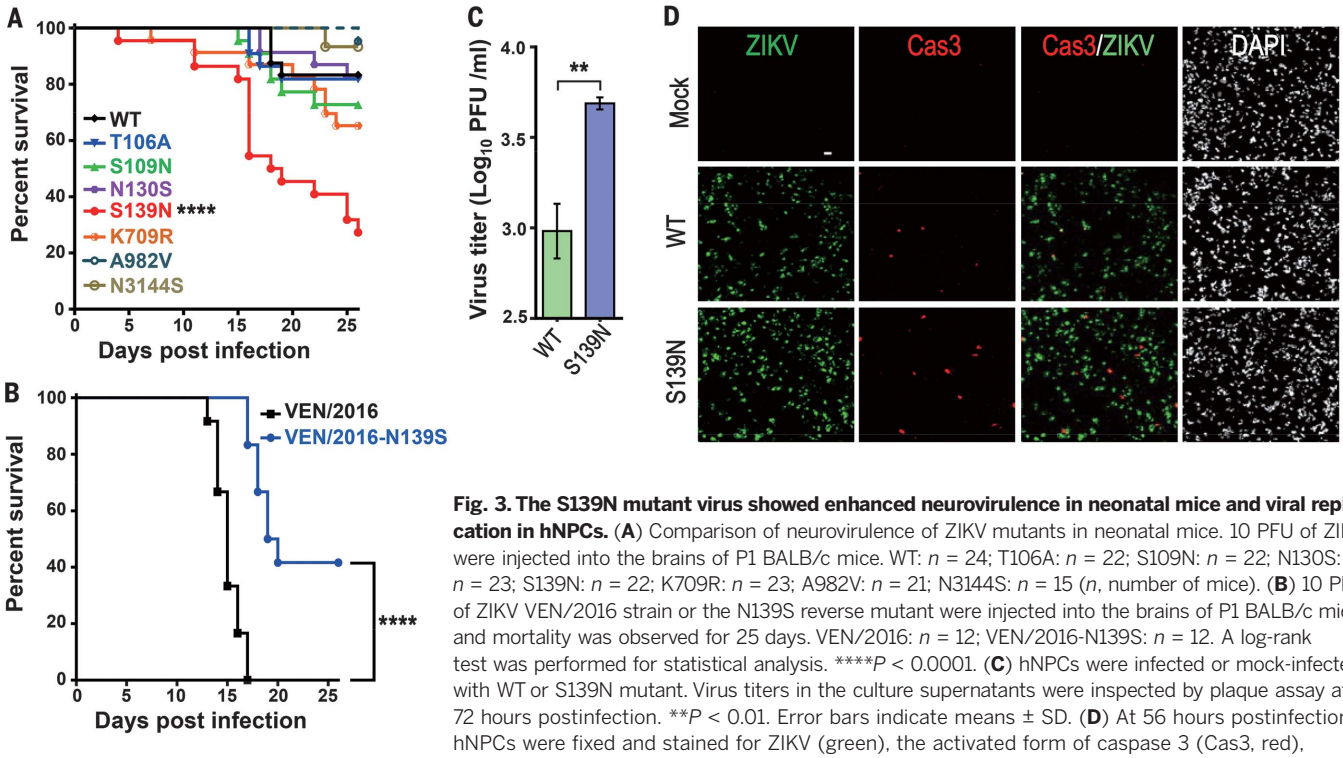

Fig. 3. The S139N mutant virus showed enhanced neurovirulence in neonatal mice and viral replication in hNPCs. (**A**) Comparison of neurovirulence of ZIKV mutants in neonatal mice. 10 PFU of ZIKV were injected into the brains of P1 BALB/c mice. WT: *n* = 24; T106A: *n* = 22; S109N: *n* = 22; N130S: *n* = 23; S139N: *n* = 22; K709R: *n* = 23; A982V: *n* = 21; N3144S: *n* = 15 (*n*, number of mice). (**B**) 10 PFU of ZIKV VEN/2016 strain or the N139S reverse mutant were injected into the brains of P1 BALB/c mice, and mortality was observed for 25 days. VEN/2016: *n* = 12; VEN/2016-N139S: *n* = 12. A log-rank test was performed for statistical analysis. ****$P < 0.0001$. (**C**) hNPCs were infected or mock-infected with WT or S139N mutant. Virus titers in the culture supernatants were inspected by plaque assay at 72 hours postinfection. **$P < 0.01$. Error bars indicate means ± SD. (**D**) At 56 hours postinfection, hNPCs were fixed and stained for ZIKV (green), the activated form of caspase 3 (Cas3, red), and 4′,6-diamidino-2-phenylindole (DAPI) (gray). Scale bar: 40 μm.

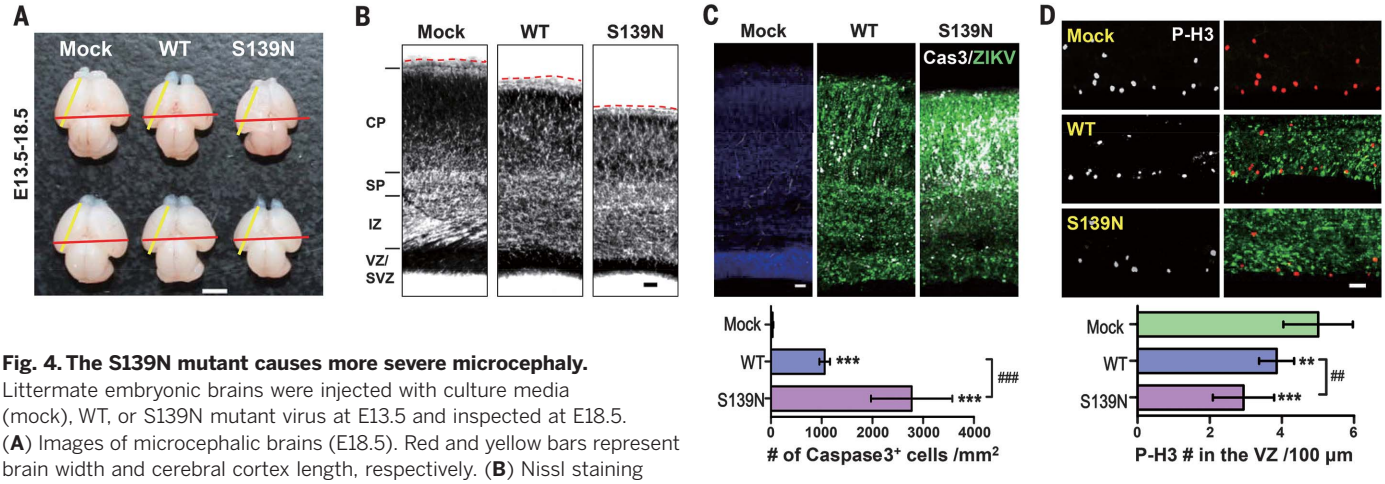

Fig. 4. The S139N mutant causes more severe microcephaly. Littermate embryonic brains were injected with culture media (mock), WT, or S139N mutant virus at E13.5 and inspected at E18.5. (**A**) Images of microcephalic brains (E18.5). Red and yellow bars represent brain width and cerebral cortex length, respectively. (**B**) Nissl staining of E18.5 brain cortices. (**C**) The S139N mutant causes more apoptosis at E18.5. (Top) Images of cortices stained with Cas3 (gray), ZIKV (green), and DAPI (blue). (Bottom) Quantification of $Cas3^+$ cells. Mock: *n* = 9/7; WT: *n* = 9/6; S139N: *n* = 10/7 (*n*, slice numbers/brain numbers). (**D**) (Top) Images of E18.5 brain cortices stained with P-H3 (red) and ZIKV (green) antisera. (Bottom) Quantification of $P\text{-}H3^+$ cells in the VZ. Mock and WT: *n* = 9/4; S139N: *n* = 13/5. All data are means ± SD (error bars); Student's *t* test. **$P < 0.01$; ***$P < 0.001$; ##$P < 0.01$; ###$P < 0.001$. Scale bars: 2 mm (A), 100 μm (B), 40 μm (C and D).

Guillain-Barré syndrome (*24*, *25*). Our findings offer an explanation for the unexpected causal link of ZIKV to microcephaly and will help to clarify how ZIKV evolved from an innocuous mosquito-borne virus into a congenital pathogen with global impact.

Structural modeling based on dengue virus, a closely related flavivirus member, indicates that residue 139, referred to as residue 17 of prM protein, is fully exposed on the surface of prM-E heterodimers or immature particles (fig. S14). The prM protein of flavivirus is required for viral maturation, egress, and secretion, and the pr domain is thought to prevent premature fusion within the infected cells (*26*). Flavivirus-infected cells contain a mixture of immature, partially mature, and mature particles (*27*). A recent study showed that the first 40 amino acids of the pr domain are involved in the interactions within trimeric spikes in the immature virus particle and affect the dynamics of conformational changes (*28*). The S139N substitution might have some effects on the transition of ZIKV from the immature to the mature virion, and the heterogeneity in maturity of progeny virions might thus affect viral fitness as well as neurovirulence. Our results also show that the ancestral Asian strain CAM/2010 can result in a mild microcephaly phenotype in mouse fetus (Fig. 1), and the N139S reverse mutant virus of contemporary ZIKV strain retains some neurovirulence to neonatal mice (Fig. 3B). Thus, further work will be required to identify additional viral genetic determinants

and host factors that might affect ZIKV pathogenesis. In addition, enhancement of vector infectivity by specific amino acid substitutions has been reported in ZIKV and other mosquito-borne viruses (*29*, *30*), but the potential relationship between epidemic potential and disease severity is still under investigation.

REFERENCES AND NOTES

1. G. W. Dick, S. F. Kitchen, A. J. Haddow, *Trans. R. Soc. Trop. Med. Hyg.* **46**, 509–520 (1952).
2. E. J. Rubin, M. F. Greene, L. R. Baden, *N. Engl. J. Med.* **374**, 984–985 (2016).
3. B. Parra *et al.*, *N. Engl. J. Med.* **375**, 1513–1523 (2016).
4. C. Li *et al.*, *Cell Stem Cell* **19**, 120–126 (2016).
5. H. Tang *et al.*, *Cell Stem Cell* **18**, 587–590 (2016).
6. K. Y. Wu *et al.*, *Cell Res.* **26**, 645–654 (2016).
7. J. J. Miner *et al.*, *Cell* **165**, 1081–1091 (2016).
8. P. P. Garcez *et al.*, *Science* **352**, 816–818 (2016).
9. S. A. Rasmussen, D. J. Jamieson, M. A. Honein, L. R. Petersen, *N. Engl. J. Med.* **374**, 1981–1987 (2016).
10. A. D. Haddow *et al.*, *PLOS Negl. Trop. Dis.* **6**, e1477 (2012).
11. N. R. Faria *et al.*, *Science* **352**, 345–349 (2016).
12. V. Heang *et al.*, *Emerg. Infect. Dis.* **18**, 349–351 (2012).
13. F. R. Cugola *et al.*, *Nature* **534**, 267–271 (2016).
14. Y. Simonin *et al.*, *EBioMedicine* **12**, 161–169 (2016).
15. F. C. Zhang, X. F. Li, Y. Q. Deng, Y. G. Tong, C. F. Qin, *Lancet Infect. Dis.* **16**, 641–642 (2016).
16. G. Piorkowski *et al.*, *New Microbes New Infect.* **11**, 52–53 (2016).
17. C. Shan *et al.*, *Cell Host Microbe* **19**, 891–900 (2016).
18. S. I. Yun *et al.*, *PLOS Pathog.* **10**, e1004290 (2014).
19. S. D. Dowall *et al.*, *PLOS Negl. Trop. Dis.* **10**, e0004658 (2016).
20. G. V. A. França *et al.*, *Lancet* **388**, 891–897 (2016).
21. J. H. Pettersson *et al.*, *mBio* **7**, e01239-16 (2016).
22. L. Wang *et al.*, *Cell Host Microbe* **19**, 561–565 (2016).
23. D. Musso, D. J. Gubler, *Clin. Microbiol. Rev.* **29**, 487–524 (2016).
24. E. Oehler *et al.*, *Euro Surveill.* **19**, 20720 (2014).
25. S. Cauchemez *et al.*, *Lancet* **387**, 2125–2132 (2016).
26. L. Li *et al.*, *Science* **319**, 1830–1834 (2008).
27. T. C. Pierson, M. S. Diamond, *Curr. Opin. Virol.* **2**, 168–175 (2012).
28. V. M. Prasad *et al.*, *Nat. Struct. Mol. Biol.* **24**, 184–186 (2017).
29. K. A. Tsetsarkin, R. Chen, M. B. Sherman, S. C. Weaver, *Curr. Opin. Virol.* **1**, 310–317 (2011).
30. Y. Liu *et al.*, *Nature* **545**, 482–486 (2017).

ACKNOWLEDGMENTS

We thank A. Davidson (University of Bristol), A.-H. Zheng (CAS), and B. Zhang (CAS) for helpful discussion and critical reagents. This work was supported by the National Natural Science Foundation of China (NSFC) (grants 31770190, 31730108, 31430037, 81661148054, and 81661130162), the National Key Research and Development Project of China (grant 2016YFD0500304), the National Science and Technology Major Project of China (grants 2017ZX09101005, 2014CB942801, and 2017ZX10304402), CAS (grants QYZDJ-SSW-SMC007 and GJHZ1827), the Shanghai Brain-Intelligence Project from the Shanghai Science and Technology Committee (grant 16JC1420500), and the Beijing Brain Project (grant Z161100002616004). C.-F.Q. was supported by an Excellent Young Scientist grant (81522025), a grant from the Innovative Research Group (81621005) from NSFC, and the Newton Advanced Fellowship from the U.K. Academy of Medical Sciences. W.S. was supported by the Taishan Scholars program of Shandong province (grant ts201511056). All data needed to understand and assess the conclusions of this research are available in the main paper and supplementary materials.

SUPPLEMENTARY MATERIALS

www.sciencemag.org/content/358/6365/933/suppl/DC1
Materials and Methods
Figs. S1 to S14
Tables S1 and S2
References (*31*–*47*)

18 January 2017; resubmitted 19 May 2017
Accepted 20 September 2017
Published online 28 September 2017
10.1126/science.aam7120

Science

A single mutation in the prM protein of Zika virus contributes to fetal microcephaly

Ling Yuan, Xing-Yao Huang, Zhong-Yu Liu, Feng Zhang, Xing-Liang Zhu, Jiu-Yang Yu, Xue Ji, Yan-Peng Xu, Guanghui Li, Cui Li, Hong-Jiang Wang, Yong-Qiang Deng, Menghua Wu, Meng-Li Cheng, Qing Ye, Dong-Yang Xie, Xiao-Feng Li, Xiangxi Wang, Weifeng Shi, Baoyang Hu, Pei-Yong Shi, Zhiheng Xu and Cheng-Feng Qin

Science **358** (6365), 933-936.
DOI: 10.1126/science.aam7120originally published online September 28, 2017

Mutation for microcephaly

Zika virus infections in humans have been known since 1947. Microcephaly and neuropathologies associated with Zika have only been reported recently, most prevalently in the Americas. Yuan *et al.* investigated recent stable mutations in the virus genome and engineered them into a low-virulence ancestral strain (see the Perspective by Screaton and Mongkolsapaya). A single amino acid substitution (serine to asparagine, S139N) in the viral precursor membrane protein exacerbated symptoms in pregnant mice. The reverse mutation (N139S) was less virulent. The S139N mutation arose in 2013 in French Polynesia before the virus jumped to Brazil in 2015. In vitro, this amino acid change made the virus more infectious for mouse and human neural progenitor cells and promoted apoptosis. The terrible sequelae of infection during pregnancy could thus be the result of a simple viral mutation.

Science, this issue p. 933; see also p. 863